Available online at www.sciencedirect.com
SCIENCE DIRECT®
Ecological Modelling 189 (2005) 1–24
ECOLOGICAL MODELLING
www.elsevier.com/locate/ecolmodel

Simulating the dynamics of primary productivity of a Sonoran ecosystem: Model parameterization and validation

Weijun Shen [a,b], Jianguo Wu [a,*], Paul R. Kemp [c], James F. Reynolds [d], Nancy B. Grimm [a]

[a] *Faculty of Ecology, Evolution and Environmental Sciences, School of Life Sciences, Arizona State University, P.O. Box 874501, Tempe, AZ 85287-4501, USA*
[b] *South China Botanical Garden, Chinese Academy of Sciences, Guangzhou 510650, PR China*
[c] *Biology Department, University of San Diego, 5998 Alcala Pk., San Diego, CA 92110, USA*
[d] *Department of Botany and Nicholas School of the Environment and Earth Science, Duke University, Durham, NC 27708-0340, USA*

Received 17 September 2004; received in revised form 30 March 2005; accepted 1 April 2005
Available online 13 June 2005

Abstract

Modeling has played a crucial role in understanding the structural and functional dynamics of forest and grassland ecosystems in the past decades, but relatively few ecosystem models have been developed for deserts. Adapting an existing desert ecosystem model to new regions with different community components and environmental settings may testify to the generality of model applicability, further verify model structure and formulations, and provide new insight into understanding desert ecosystem functioning. In this paper, we use a desert ecosystem model that was originally developed for the Chihuahuan Desert, Patch Arid Land Simulator-Functional Types (PALS-FT), to estimate the aboveground annual net primary productivity (ANPP) of a creosotebush (*Larrea tridentata*)-dominated Sonoran Desert ecosystem in the Phoenix metropolitan area, home to the Central Arizona-Phoenix Long-Term Ecological Research Project (CAP LTER). We modified and parameterized the model using meteorological data, ecophysiological parameters for different plant functional types, and site characteristic data from the CAP LTER study area and an independent test site in the San Simon Valley of southeastern Arizona. Model predictions were validated and calibrated using field observations from the San Simon Valley test site. The results showed that PALS-FT was able to simulate ANPP of this typical Sonoran Desert ecosystem reasonably well, with a relative error of ±2.4% at the ecosystem level and generally less than ±25% at the functional-type level. We then used the model to simulate ANPP and its seasonal and inter-annual dynamics for a similar ecosystem in the CAP LTER study area. The model predicted average annual ANPP of 72.3 g m^{-2} y^{-1}, ranging from 11.3 g m^{-2} y^{-1} to 229.6 g m^{-2} y^{-1} in a 15-year simulation. The simulated average ANPP of the Sonoran Desert ecosystem is close to field observations in other areas of the Sonoran Desert, and the range of variation also is close to that reported by other researchers for arid and semiarid ecosystems. The dynamics of ecosystem ANPP in response to fluctuations in

* Corresponding author. Tel.: +1 480 965 1063; fax: +1 480 965 6899.
E-mail address: jingle.wu@asu.edu (J. Wu).

0304-3800/$ – see front matter. Published by Elsevier B.V.
doi:10.1016/j.ecolmodel.2005.04.010

annual precipitation simulated by the model agreed well with the known relationship between ANPP and precipitation in arid and semiarid systems. A closer examination of this relationship at the level of plant functional types further revealed that seasonal distribution of rainfall significantly affected ANPP. A comparison between the PALS-FT model prediction and two regression models for North American warm deserts showed that both regression models underestimated the *Larrea* ecosystem ANPP, while the process-based PALS-FT model provided the most accurate prediction among the three models. This study provides a validation for use of the PALS-FT model to investigate Sonoran desert ecosystem responses to environmental changes.
Published by Elsevier B.V.

Keywords: Net primary productivity; Sonoran Desert; *Larrea*; PALS-FT; Model parameterization; Model validation; Long-term ecological research

1. Introduction

Arid and semiarid regions occupy over one third of the world's land surface and are home to more than 20% of the global human population (Reynolds and Smith, 2002). Many drylands have been degraded by overcultivation, overgrazing, fuel gathering, urbanization, and climate change (Schlesinger et al., 1990; Wu, 2001; Reynolds and Smith, 2002). With the accelerating rate of desertification around the world, especially in Africa and central Asia, the capacity of arid lands to support humans, livestock, and wild animals is decreasing substantially. Understanding the basic functioning of desert ecosystems is thus of paramount importance to combating desertification and supporting sustainable use of arid land. An important indicator of ecosystem functioning is aboveground net primary productivity. It not only reflects how well the primary producers of an ecosystem are growing, but also indicates the amount of energy available to consumers and decomposers that, in turn, drive other important ecosystem processes (e.g. biogeochemical cycles, decomposition). The primary production of desert ecosystems has been a major research topic for decades (Noy-Meir, 1973; Fischer and Turner, 1978; Hadley and Szarek, 1981; Ludwig, 1987; Whitford, 2002). Studies have investigated water-use efficiency (Webb et al., 1978; LeHouerou et al., 1988), below-ground productivity (Caldwell and Camp, 1974; Bell et al., 1979), relationships between productivity and rainfall variability (Ludwig, 1986; LeHouerou et al., 1988), and productivity of individual species or functional groups (Chew and Chew, 1965; Burk and Dick-Peddie, 1973; Whittaker and Niering, 1975; Johnson et al., 1978; Reynolds et al., 1980, 1997; Fisher et al., 1988; Turner and Randall, 1989). While these studies, based on field observations and measurements, provide valuable insight into desert ecosystem processes, the generally short duration of the studies often limits the ability to obtain a clear understanding of cause and effect relationship that govern productivity in these highly temporally variable ecosystems. Thus, ecosystem simulation is a potentially powerful tool to aid in the understanding of ecosystem functioning, especially with respect to temporal processes such as climate variability and atmospheric change (e.g. changes in precipitation patterns, CO_2, N deposition), as well as other human perturbations and management activities. However, model development with respect to desert ecosystems has lagged behind that compared with some other ecosystems, e.g. forest and grasslands (see Tiktak and van Grinsven, 1995; Ryan et al., 1996; Parton et al., 1996).

Models for estimating terrestrial ANPP can be categorized into three types: statistical models, parametric models, and process models (Reynolds et al., 1993; Ruimy et al., 1994), in which process-based models are generally considered to be more useful for understanding the mechanisms of plant growth and plant-environment interactions, and for extrapolating predictions of ecosystem responses to environmental changes. Most ecosystem models for desert ecosystems are either statistical (e.g. Noy-Meir, 1973; Webb et al., 1978; LeHouerou et al., 1988) or process models (e.g. Reynolds et al., 1980, 1997; Reynolds and Cunningham, 1981). The Patch Arid Land Simulator-Functional Types (PALS-FT) is a mechanistic process-based model developed originally for the Chihuahuan Desert ecosystem in the Jornada Basin, New Mexico, USA (Reynolds et al., 1997). It has been used to study effects of disturbances on grassland-shrubland transition (Gao and Reynolds, 2003), effects of rainfall variability on canopy transpiration and soil water dynamics (Reynolds et al., 2000), and ecosystem responses to climate change in the

Chihuanhuan Desert (Reynolds et al., 1997). Applying the model and expanding these studies to new regions, longer time frames, and/or new types of environmental changes (e.g. urbanization-induced environmental changes) can further verify the structural rationality and predictive accuracy of the model and provide new insight into desert ecosystem functioning.

As part of the effort to understand and predict how urbanization affects ecosystem processes in metropolitan Phoenix, Arizona, USA, a city in the Sonoran Desert (see Grimm et al., 2000), the main objective of this study was to adapt and evaluate the PALS-FT model for the Sonoran desert, which boasts the highest plant diversity among the four North American Deserts (Sonoran, Chihuahuan, Mojave, and the Great Basin). This is due in part to the presence of both summer and winter showers in the Sonoran Desert compared to predominately summer rainfall in the Chihuanhuan Desert and winter rainfall in the Great Basin and Mojave Deserts (Brown, 1994; MacMahon, 2000). Specifically, we sought to determine whether the PALS-FT model can be applied to simulate the ecosystem ANPP of the *Larrea* dominated Sonoran Desert ecosystem with acceptable accuracy and consistency against field observations. We first briefly describe the structure and formulations of the PALS-FT model including modifications for application to the Sonoran Desert. The model parameter development and evaluation was accomplished using data from an independent testing site in the southeastern Sonoran Desert. The model was then used to examine seasonal and inter-annual patterns of ANPP in response to precipitation fluctuations over the northwest CAP study area of the Sonoran Desert. The PALS-FT model predictions were also compared with those of regression models that had been developed for the North American hot deserts, and the potential uses of the model to investigate urbanization effects on desert ecosystem function are discussed.

2. Model description

PALS-FT is a physiologically based ecosystem model that simulates the dynamics of carbon (C), nitrogen (N), and water (H_2O) cycling of a desert ecosystem in a daily time step, with explicit consideration of plant functional types (FTs) of shrub, subshrub, perennial grasses, forbs, C3 winter-annual, and C4 summer-annual species (Reynolds and Cunningham, 1981; Reynolds et al., 1993, 1997, 2000; Kemp et al., 1997). The model was developed based on the hypothesis that changes in ecosystem structure and function are determined primarily by the dynamics of different plant FTs and soil resource distributions (Reynolds et al., 1997). PALS-FT consists of four interacting modules: (i) atmospheric driving variables and surface energy budget, (ii) soil water distribution and water cycling, (iii) production of plant FTs, and (iv) nutrient (C, N) cycling. PALS-FT is similar to patch-dynamic models (e.g. Shugart, 1984; Wu and Levin, 1994, 1997) in that it simulates ecological processes on a "patch" of certain size. The patch size used for PALS is variable, depending upon the desired resolution, FT composition, and interaction among adjacent patches. Previous studies using PALS-FT considered relatively small patch sizes (ca. 1–30 m^2) in order to investigate small-scale spatial heterogeneity along a topographic gradient (Reynolds et al., 1997, 2004; Gao and Reynolds, 2003). But in this study, we treated the "patch" as a generalized ecosystem unit at the scale of 1–100 km^2 for the purpose of representing a geographic area with relatively homogeneous abiotic conditions and similar ecosystem components. Model inputs and initialization includes data on climatic conditions, soil physical properties, plant and soil C and N storage, and plant ecophysiological parameters. Major model output variables include ANPP, soil evaporation, canopy transpiration, vegetation cover, soil organic matter, and soil C and N mineralization. Because PALS-FT has already been described in previous studies (Reynolds et al., 1997, 2000, 2004), we provide only an overview of the general model, focusing on the elements that were modified or are particularly relevant to the objectives of our study.

2.1. Atmospheric driving variables and surface energy budget

This module includes inputs of environmental driving variables (e.g. daily precipitation, maximum and minimum temperatures, solar radiation, relative humidity, ambient CO_2 concentration, and N deposition rate) and the calculation of other environmental variables using these input driving variables (e.g. day length or photoperiod, mean air temperatures, soil temperature, and vapor pressure deficit (VPD).

Photoperiod is calculated as a cosine function of Julian day:

$$\text{Photoperiod} = 12 + 2\cos\left(\pi \times \left(\frac{\text{Julian day} - 172}{182.5}\right)\right) \quad (1)$$

VPD, an important variable in determining stomatal conductance, is the difference between saturated vapor pressure (VP_{sat}) and measured vapor pressure (VP_{air}) corresponding to maximum air temperature (T_{max}, in °C), i.e.

$$VPD(T_{max}) = VP_{sat}(T_{max}) - VP_{air} \quad (2)$$

and

$$VP_{sat}(T_{max}) = 0.611 \times 10^{((7.5\times T_{max})/(237.3+T_{max}))} \quad (3)$$

$$VP_{air} = rh \times VP_{sat}(T_{max}) \quad (4)$$

where rh is the relative humidity (%).

Surface soil temperature (at 1 cm depth) is estimated using the following empirical equations:

$$ST_{max} = T_{max} + 0.962 \times R_s - 6.63 \quad (5)$$

$$ST_{min} = T_{min} - 0.55 \quad (6)$$

$$ST_{avg} = \frac{0.77 \times ST_{max} + ST_{min}}{2} \quad (7)$$

where ST_{max}, ST_{min} and ST_{avg} are the maximum, minimum and average surface soil temperature (°C), respectively, T_{max} and T_{min} are the maximum and minimum air temperature (°C), respectively, and R_s the total solar radiation (MJ m^{-2} day^{-1}).

The belowground average daily soil temperature is calculated for a relatively deep point (200 cm) using a sinusoidal function given by Campbell (1977; equation 2.8) with a mean annual deep soil temperature of 20 °C (200 cm), a surface (−1 cm) annual amplitude of mean daily temperature of 13.7 °C, and an average annual damping depth of 170 cm (which corresponds to an average thermal diffusivity of 0.003 cm^2/s) and a phase adjustment of 91 Julian days for occurrence of mean daily surface (−1 cm) temperature. This same equation is used to calculate the soil temperature at a shallow point (50 cm) by including a site-specific harmonic term to account for asymmetry nearer the surface. Soil temperatures at depths from the surface to 50 cm are determined by interpolation of the logarithmic decay the surface temperature (Eq. (7)) to the predicted daily mean temperature at 50 cm; and soil temperatures from 50 to 200 cm are predicted by interpolation of the logarithmic decay between these two depths.

2.2. Soil water distribution and water cycling module

The water cycling module simulates daily soil evaporation, plant transpiration, and water content and movement in different soil layers (Fig. 1). The water reaching the soil surface of the patch, "effective precipitation" (EP, in cm d^{-1}), is estimated as a function of actual precipitation (Ppt), interception, run on, and run off, i.e.

$$EP = Ppt - intcpt + runon - runoff \quad (8)$$

$$intcpt = SS \times 2 \times LAI_t \quad (9)$$

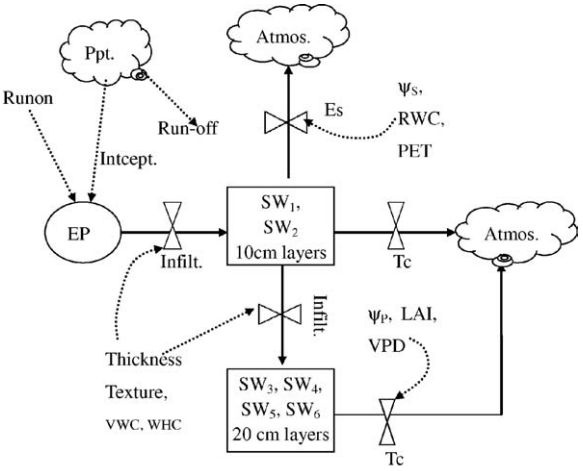

Abbreviation	Description	Unit
Atmos.	Atmosphere	
Ppt.	Precipitation	cm
Intcept.	Interception	cm
Infilt.	Infiltration	cm d^{-1}
LAI	Leaf area index	m^2 m^{-2}
PET	Potential evapotranspiration	cm
WHC	Water holding capacity	cm
VWC	Volumetric water content	%
VPD	Vapor pressure deficit	kPa
SW_i	Soil water content at layer i	cm
Es	Evaporation	cm d^{-1}
Tc	Canopy transpiration	cm d^{-1}
ψ_p	Water potential of plant	kPa
ψ_s	Water potential of soil	kPa

Fig. 1. Flow diagram for water cycling and soil water distribution processes in the PALS-FT model.

where SS is the surface storage of water film on foliage (ave. for all FTs is ca. 0.02 cm; Reynolds et al., 2000), 2 is a factor accounting for the two sides of the leaf, and LAI_t is the total leaf area index ($m^2\,m^{-2}$) including all plant functional types (as in Kemp et al., 1997). Water run-on and run-off in the simulated patch were not considered because of the negligible slope (<1%) in northwestern Phoenix and our testing site (Fig. 4).

Soil water is represented in 6 layers in the PALS-FT model: the upper two layers with a depth of 10 cm each and the other 4 layers with a depth of 20 cm each. Water infiltration of each layer is determined by the amount of water percolating out of the upper layer, previous water content, and water holding capacity (WHC) of the layer. Water is removed from the two top layers by evaporation and from all layers by transpiration. Evaporation is determined by soil water availability (soil water potential and relative water content, RWC) and energy available at the soil surface. Water taken up by plants is partitioned among the soil layers according to the proportions of roots in each layer for all FTs. Actual canopy transpiration is estimated by a simple energy budget model and a canopy stomatal resistance function (Kemp et al., 1997; Reynolds et al., 2000).

2.3. Plant production module

PALS-FT's plant production module simulates plant phenology, growth, and C allocation to different plant parts (Fig. 2). Plant growth, litter fall, and plant mortality are influenced by FT-specific patterns of phenology that are controlled by water availability and extreme temperatures. The plant production module for C3 and C4 annuals and perennial grasses differs slightly from Fig. 2 in its inclusion of seed germination and reproduction for the annual FTs and regrowth from roots/rhizomes for grasses. The amount of daily plant growth for all FTs (G_j, in g dry mass m^{-2}) is calculated in the same way:

$$G_i = X_{\mathrm{lvs}} \times \mathrm{SLA} \times A_{\mathrm{max},j} \times \frac{12}{0.46} \times (1 - R_{\mathrm{loss}}) \times F_{\mathrm{c}} \times F_{\mathrm{t}} \quad (10)$$

where X_{lvs} is the leaf dry mass (g), SLA the specific leaf area ($m^2\,g^{-1}$), $A_{\mathrm{max},j}$ the maximum potential net photosynthetic rate (mol CO_2 $m^{-2}\,s^{-1}$), the value of 12 is the mass of 12 g C/mol CO_2, 0.46 is the average C content (46%) in plant tissues, R_{loss} the respiratory loss of photosynthetic production per day, F_{t} the temperature influence factor (for forbs and grasses, not for shrubs), and F_{c} (=$2/\pi \times$ photoperiod $\times$ 3600) is a conversion factor (changing time unit from second to day; Monteith and Unsworth, 1990). The annual growth of plants calculated from Eq. (10) can be summed over the year (or season for annual FTs) and reduced by allocation to above-ground plant material to obtain a measure of aboveground net primary productivity (ANPP; herbivory is considered insignificant in the model).

$A_{\mathrm{max},j}$ is estimated using the following equation (Ehleringer, 1983):

$$A_{\mathrm{max},j} = \frac{g_j}{1.6} \times \frac{\mathrm{Ca} - \mathrm{Ci}_j}{p} \quad (11)$$

where g_j is the stomatal conductance (mol H_2O $m^{-2}\,s^{-1}$), Ca the partial pressure of atmospheric CO_2 concentration (kPa), and Ci_j the partial pressure of intercellular CO_2 (kPa), 1.6 is the ratio of diffusivity of H_2O (21.2×10^{-6}) to CO_2 (12.9×10^{-6}), p is the atmospheric vapor pressure (kPa) The value of Ci_j is assumed to be determined by the physiological/anatomical capacity of each FT ($Ci_{\mathrm{min},j}$), and is assumed to be affected by leaf N levels (S_j^{N}):

$$\mathrm{Ci}_j = \mathrm{Ca} - (\mathrm{Ca} - \mathrm{Ci}_{\mathrm{min},j}) \times S_j^{\mathrm{N}} \quad (12)$$

and S_j^{N} is a linear scalar accounting for the effect of leaf N on Ci_j of FT_j. S_j^{N} is defined as:

$$S_j^{\mathrm{N}} = \begin{cases} 1 & if\ N_{\mathrm{L}} > 1 \\ 0.1 & if\ N_{\mathrm{L}} < 0.1 \\ \dfrac{N^{\mathrm{leaf}} - N_{\mathrm{min}}^{\mathrm{leaf}}}{N_{\mathrm{max}}^{\mathrm{leaf}} - N_{\mathrm{min}}^{\mathrm{leaf}}} (= N_{\mathrm{L}}) & if\ 0.1 \le N_{\mathrm{L}} \le 1 \end{cases} \quad (13)$$

where N^{leaf} is the currently simulated leaf N fraction, and $N_{\mathrm{max}}^{\mathrm{leaf}}$ and $N_{\mathrm{min}}^{\mathrm{leaf}}$ are the maximum and minimum possible leaf N fractions. Calculation of A_{max} requires a value for stomatal conductance (g_j). While many photosynthesis models employ schemes for predicting g in relation to feedback from carbon uptake (e.g. Ball et al., 1987; Leuning, 1995), other successful stomatal models have considered that g is a function of leaf water potential, VPD, light, or temperature (e.g. Jarvis, 1976; Oren et al., 1999). The PALS-FT model assumes that the overriding factors controlling stomatal conductance

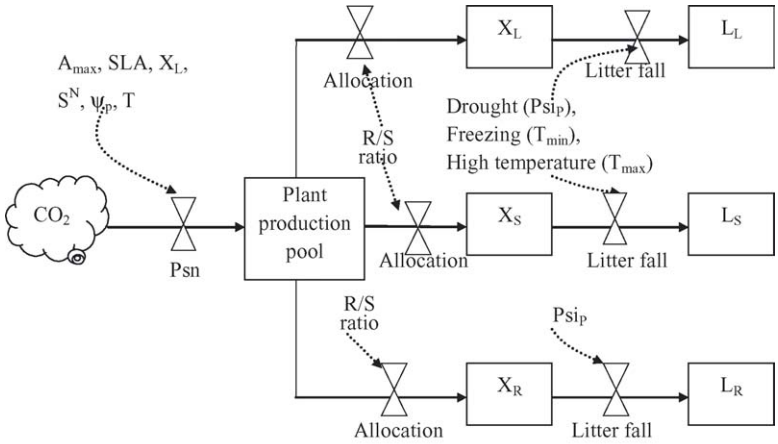

Abbreviation	Description	Unit
X_L	Leaf biomass	g DM m^{-2}
X_S	Stem biomass	g DM m^{-2}
X_R	Root biomass	g DM m^{-2}
L_L	Leaf litter	g DM m^{-2}
L_S	Stem litter	g DM m^{-2}
L_R	Root litter	g DM m^{-2}
Psn	Photosynthetic rate	g DM m^{-2} d^{-1}
A_{max}	Maximum potential net photosynthetic rate	mol CO_2 m^{-2} s^{-1}
DM	Dry mass	g
SLA	Specific leaf area	m^2 g^{-1}
ψ_P	Water potential of plant	kPa
Psi_P	$-\psi_P$	kPa
T	Temperature	℃
R/S	Root-shoot ratio	Fraction
S^N	Scalar for N effects	Fraction

Fig. 2. Schematic diagram of plant production module for shrubs in the PALS-FT model.

in desert plants is plant water potential (leaf hydration) and atmospheric vapor deficit (see Kemp et al., 1997). Thus, g_j is calculated as an exponential function of FT leaf water potential (Ψ_j) with a linear relationship to decreasing atmospheric vapor deficit (VPD in kPa):

$$g_j = a \times e^{(b \times \Psi_j)} \times (1 - 0.1 \times \text{VPD}) \quad (14)$$

with a and b as FT-specific parameters defining the exponential decline in g_j with decreasing Ψ_j (Table A.2). A daily value for leaf water potential of each FT (Ψ_j) is calculated from the water potential of all soil layers weighted by the fraction of roots of each FT in each specific layer (see Kemp et al., 1997).

2.4. Nutrient cycling module

The nutrient cycling module simulates the dynamics of C and N in the soil-plant-atmosphere system (Fig. 3), and is a modified version of the nutrient cycling part of the CENTURY model (Parton et al., 1988, 1993). Three kinds of plant litter are distinguished for each of the FTs: leaf litter, stem litter, and root litter; with the leaf and stem litter being allocated to one of two chemical pools on the soil surface (metabolic or structural C) and root litter being allocated to one of two pools in the belowground soil (also metabolic or structural C). The partitioning of litter into metabolic or structural fractions was based on literature values of residual chemical composition

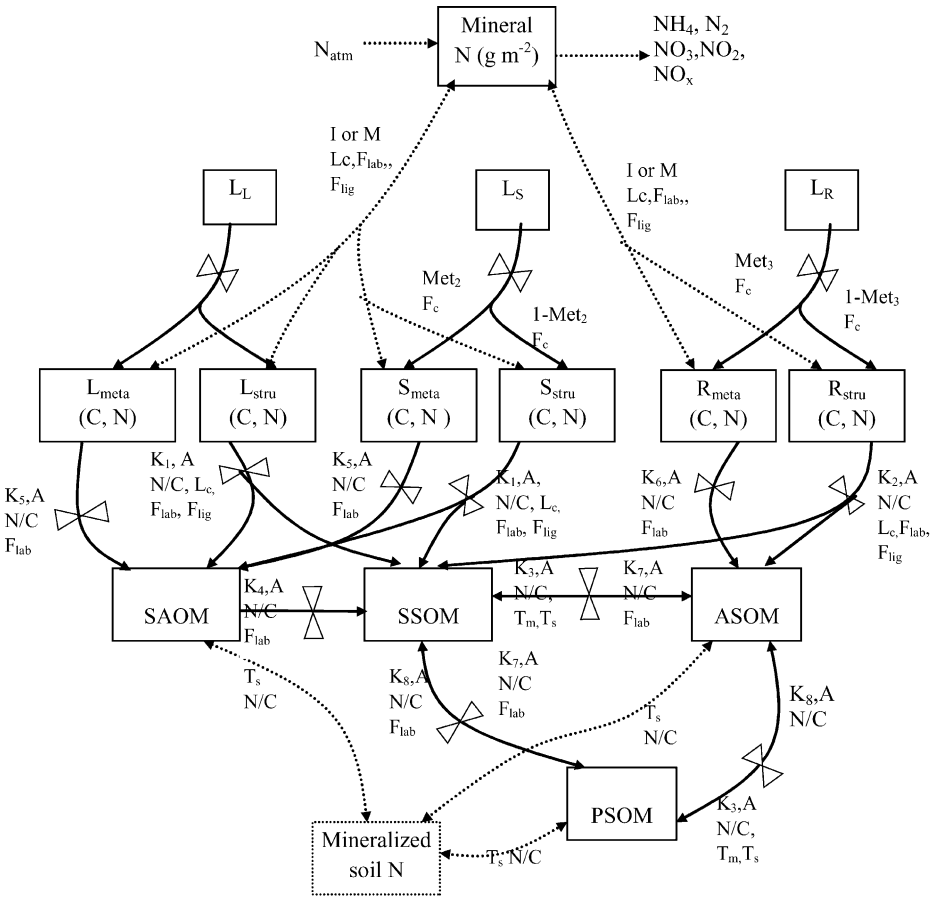

Abbreviation/ Symbol	Description	Unit	Abbreviation/ Symbol	Description	Unit
----------	Only nitrogen flow		N_{atm}	Atmospheric N deposition	g m^{-2} d^{-1}
———	Both C and N flow		NH_4, N_2, NO_x	Mineral Nitrogen	g m^{-2}
L_L	Leaf litter	g DM m^{-2}	K_i, i= 1, 2, ---, 8	Decomposition rates	day^{-1}
L_S	Stem litter	g DM m^{-2}	I	Immobilization	
L_R	Root litter	g DM m^{-2}	M	Mineralization	
L_{meta}	Leaf metabolic C, N	g m^{-2}	N/C	Ratio of nitrogen to carbon	
L_{stru}	Leaf structural C, N	g m^{-2}	Met_i i= 1, 2, ---, 4	Fraction of metabolic material in litter mass	
S_{meta}	Stem metabolic C, N	g m^{-2}	L_c	Effect of lignin content on decomp	
S_{stru}	Stem structural C, N	g m^{-2}	A	Effect of soil abiotic condition on decomposition	
R_{meta}	Root metabolic C, N	g m^{-2}	T_m	Effect of soil texture on ASOM turnover	
R_{stru}	Root structural C, N	g m^{-2}	T_s	Effect of soil texture on organic N decomposition	
SAOM	Surface active organic matter	g m^{-2}	F_c	Fraction of carbon in litter mass	
SSOM	Slow soil organic matter	g m^{-2}	F_{lab}	Fraction of N mineralized from labile material	
ASOM	Active soil organic matter	g m^{-2}	F_{lig}	Fraction of N mineralized from lignin and cellulose	
PSOM	Passive soil organic matter	g m^{-2}			

Fig. 3. Schematic diagram of nutrient cycling module in the PALS-FT model.

of litter types for each FT (see Kemp et al., 2003):

$$\frac{dC_{m,i}}{dt} = \sum_{j=1}^{6} \frac{dL_{i,j}}{dt} \times \text{Met}_{i,j} \times F_{c,j},$$

for metabolic material (15)

$$\frac{dC_{s,i}}{dt} = \sum_{j=1}^{6} \frac{dL_{i,j}}{dt} \times (1 - \text{Met}_{i,j}) \times F_{c,j}$$

for structural material (16)

where $i = 1, 2, 3$ for leaf, stem and root, $j = 1, 2, 3, 4, 5, 6$ for the 6 plant functional types, $C_{m,i}$ and $C_{s,i}$ are the C contents (g) in metabolic and structural material, respectively, $L_{i,j}$ is the litter dry mass in each litter type i-FT_j combination, $\text{Met}_{i,j}$ is the fraction of metabolic material, and $F_{c,j}$ is the fraction of C content of litter type i (in dry mass) of FT_j.

The input rates of N from plant litter to metabolic (N_m) and structural material (N_s) pools are modeled similarly to C:

$$\frac{dN_{m,i}}{dt} = \left(\sum_{j}^{6} \frac{dL_{i,j}}{dt} \times N_{i,j} \right) - \frac{dN_{s,i}}{dt},$$

for metabolic material (17)

$$\frac{dN_{s,i}}{dt} = \sum_{j=1}^{6} \frac{dL_{i,j}}{dt} \times (1 - \text{Met}_{i,j}) \times F_{c,j} \times \left(\frac{N}{C} \right)_{i,j},$$

for structural material (18)

where i, j, $L_{i,j}$, $F_{c,j}$, and $\text{Met}_{i,j}$ are the same as in Eqs (15) and (16), $N_{i,j}$ is the N content (% of dry mass) of litter type i of FT_j, and $(N/C)_{i,j}$ is the ratio of N to C for litter type i of FT_j.

After decomposition, the metabolic and structural material of plant litter enters into one of the three soil organic matter (SOM) pools: surface litter enters the surface active organic matter (SAOM), and belowground litter enters the active soil organic matter (ASOM) or slow soil organic matter (SSOM) according to the partitioning scheme employed in CENTURY (Parton et al., 1993), and a small fraction of the C from the soil organic matter pools enters the passive soil organic matter (PSOM). The flows of C from metabolic and structural material pools to the three SOM pools and among the SOM pools are depicted in Fig. 3 and are defined by the following differential equations (Parton et al., 1993):

$$\frac{dC_i}{dt} = K_i \times L_C \times A \times C_i, \quad i = 1, 2 \tag{19}$$

$$\frac{dC_i}{dt} = K_i \times A \times T_m \times C_i, \quad i = 3 \tag{20}$$

$$\frac{dC_i}{dt} = K_i \times A \times C_i, \quad i = 4, 5, 6, 7, 8 \tag{21}$$

where C_i is the C in the state variable i; $i = 1, 2, 3, 4, 5, 6, 7, 8$ denote surface (leaf and stem) structural material, root structural material, active soil organic matter, surface-active organic matter, surface metabolic material, soil metabolic material, slow soil organic matter fractions, and passive soil organic matter fractions, respectively; K_i is the maximum decomposition rate (day^{-1}) for the ith state variable (Table A.1); L_C the impact of lignin content of structural material on its decomposition, T_m is the effect of soil texture on ASOM turnover, and A is the combined abiotic impact of soil moisture and soil temperature on decomposition (product of the soil moisture and temperature terms). Calculations of L_C, T_m, and A are as in Parton et al. (1993).

The dynamics of N in decomposing organic matter is coupled directly to the flows of C through the various SOM pools. The flow of N among these pools is equal to the product of the C flows and the N/C ratio of the recipient state variable (Parton et al., 1993). Specifically, the following differential equations describe the dynamics of organic N among different pools:

$$\frac{dN_i}{dt} = \left(1 - \left(\frac{L}{S}\right)_i\right) \times (1 - F_{\text{lab,min}}) \times \frac{dC_i}{dt} \times \left(\frac{N}{C}\right)_i + \left(\frac{L}{S}\right)_i \times (1 - F_{\text{lig,min}}) \times \frac{dC_i}{dt} \times \left(\frac{N}{C}\right)_i \quad i = 1, 2 \tag{22}$$

$$\frac{dN_i}{dt} = (1 - T_m) \times \frac{dC_i}{dt} \times \left(\frac{N}{C}\right)_i \quad i = 3 \tag{23}$$

$$\frac{dN_i}{dt} = (1 - F_{lab,min}) \times \frac{dC_i}{dt} \times (N/C)_i \quad i = 4, 5, 6, 7, 8 \tag{24}$$

where N_i is N in state variable i; i represent the same organic pools as in Eqs. (19)–(21); $(L/S)_i$ the ratio of lignin content to the summation of lignin and cellulose material in the ith organic pool (Table A.2); $(N/C)_i$ the ratio of N to C for the ith organic matter pool and calculated in each time step of simulation; $F_{lab,min}$ is the fraction of N in labile material lost due to microbial respiration (Table A.2); $F_{lig,min}$ is the fraction of N in non-labile material (i.e. lignin and cellulose) lost due to microbial respiration (Table A.2); T_s the effect of soil texture on organic N turnover (Parton et al., 1993).

For different organic matter pools, N associated with C lost in respiration is assumed to be mineralized. Nitrogen mineralization rates are also the products of the decomposition rates (dC_i/dt) of corresponding carbon pools, the fraction of respiratory N loss ($F_{lab,min}$), and N/C ratio. Thus, we have:

$$\frac{dN_{i,min}}{dt} = \left(1 - \left(\frac{L}{S}\right)_i\right) \times (F_{lab,min}) \times \frac{dC_i}{dt} \times \left(\frac{N}{C}\right)_i + \left(\frac{L}{S}\right)_i \times (F_{lig,min}) \times \frac{dC_i}{dt} \times \left(\frac{N}{C}\right)_i \quad i = 1, 2 \tag{25}$$

$$\frac{dN_{i,min}}{dt} = T_s \times \frac{dC_i}{dt} \times \left(\frac{N}{C}\right)_i \quad i = 3, 4 \text{ if } \frac{N}{C} > \frac{1}{8}, \text{ or } i = 7, 8 \text{ if } \frac{N}{C} > \frac{1}{11}, \text{ otherwise, } \frac{dN_{i,min}}{dt} = -0.02 \tag{26}$$

$$\frac{dN_{i,min}}{dt} = F_{lab,min} \times \frac{dC_i}{dt} \times \left(\frac{N}{C}\right)_i \quad i = 5, 6 \tag{27}$$

where $N_{i,min}$ is the N loss from the ith organic matter pool through mineralization, and all other parameters are the same as in Eqs. (22)–(24).

3. Model parameterization

The study area is located northwest of Phoenix, Arizona, USA, within the Central Arizona-Phoenix Long Term Ecological Research (CAP LTER) study area (Fig. 4). The Sonoran Desert scrub biome occupies most of southwestern Arizona below 1050 m (Turner and Brown, 1994). Shreve (1951) recognized seven vegetation subdivisions in the Sonoran Desert, two of which occur in the CAP LTER study area: Lower Colorado River Valley subdivision and Arizona upland subdivision. The lower Colorado River Valley subdivision occupies most of the CAP LTER study area, particularly in the northwestern portion, and is dominated by creosotebush (*Larrea tridentata*) and triangle-leaf bursage (*Ambrosia deltoidea*; Turner and Brown, 1994; MacMahon, 2000). The Arizona upland subdivision occurs in the northeastern part of the CAP LTER study area and is dominated by paloverde (*Cercidium microphyllum*) and cacti (*Carnegiea gigantea*, *Opuntia spp*), with creosotebush and bursage common as well. The rest of the CAP LTER study area is composed mainly of agricultural, urban, and riparian lands. In this study, we focus on the *Larrea* and *Ambrosia* co-dominated communities.

We have classified input data to PALS-FT into two groups: site-specific parameters and plant-ecophysiological parameters. Site parameters include climatic variables, living and dead plant biomass (initial values of state variables), and soil properties (e.g. texture, organic matter content) (Table A.1). The plant-ecophysiological parameters include distribution of plant root fractions in different soil layers, specific leaf area, respiratory loss ratios of daily production, minimum leaf intercellular CO_2, contents of N, C, lignin and cellulose in leaves, stems and roots, and production allocation ratios (Table A.2). The two kinds of parameter values were obtained from three sources: the CAP LTER 200-point field survey data, literature, and values used in the original PALS-FT model. The 200-point survey data were the major source for site-specific parameters, although climatic data were obtained from the Wadell Weather Station, which is located in the northwest fringe of metropolitan Phoenix about 50 km from the urban center (Fig. 4).

The 200-point survey data were obtained from an extensive field survey with 204 sample plots (30 m × 30 m) throughout the metropolitan area,

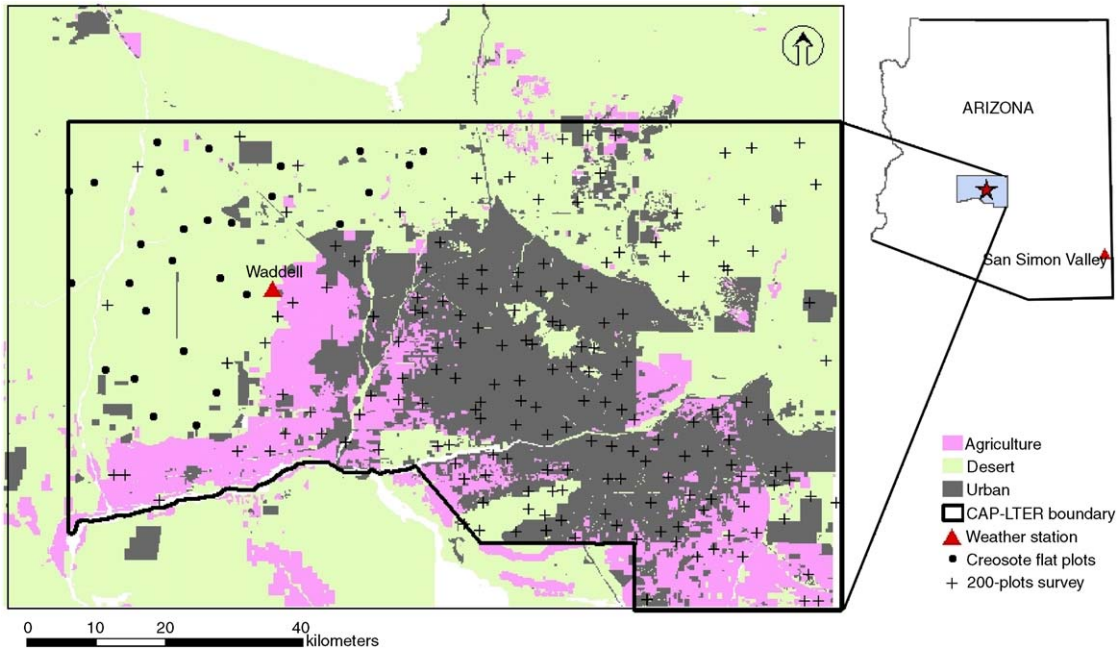

Fig. 4. Maps showing the research sites of this study. Solid dots represent sampling plots of the *Larrea* ecosystem in the CAP LTER research area. Solid triangles represent the positions of weather stations from where the meteorological data were obtained for driving the PALS-FT model. The San Simon Valley is site of Chew and Chew's (1965) field study of biomass and NPP of a *Larrea* ecosystem, which was used to validate the model.

which was carried out by CAP LTER over a 3-month period in spring 2000 (Hope et al., 2003). In order to obtain a spatially dispersed and unbiased sample that allows for maximum post-design extrapolation, a dual-density randomized tessellation stratified design was used to locate the sample plots. At each location, a systematic, integrated field inventory of key abiotic, biotic, and human variables was carried out. Within each plot all woody plants (trees, shrubs, cacti, succulents) were identified, and the canopy dimensions of each individual measured to give the total volume of woody plant material. Five soil cores were taken at each site, which each were separated into 0–10 cm and 11–30 cm sections. Soil samples were analyzed to determine moisture content, organic matter content, bulk density, particle size distribution, pH, readily leachable soil nitrate and phosphate content, and inorganic and organic C content. Other measured variables included meteorological conditions, land-use and land-cover types, insect populations, surface pollens, and prokaryote and mycorrhizal diversity. In addition, information was also obtained on elevation, distance from urban center, distance from the nearest major freeway, land-use history, median family income, average age of housing stock, and human population density.

PALS-FT distinguishes between living and dead biomass. The 200-point survey data only provide total vegetation cover for each plot. In order to estimate the biomass of each of the six plant functional types, we first derived an average vegetation coverage (32.9%) based on the measures in 30 of the 204 plots (see Fig. 4), and then calculated the plant cover of individual FTs as the product of the average total cover and the relative cover of each FT which was measured in the same area by Camp (1986). Then, the total aboveground biomass of each FT was estimated based on empirical cover-biomass relations (Table 1). Further, the biomass of leaves, stems, and roots of perennial FTs (i.e. perennial grass, subshrub and shrub) was calculated using biomass-allocation ratios derived from Chew and Chew (1965). The dead biomass was calculated according to the dead to living biomass ratio used in the original PALS-FT model. Plant litter is split into metabolic and structural material. We estimated the size of the two

Table 1
Species composition, vegetation cover, and biomass of different plant functional types in the *Larrea* community in northwestern Phoenix

Functio-nal type	Plant species	Relative cover[a] (%)	Ground cover (%)	Cover-biomass relation[b]	Above-ground biomass (AGB, g m^{-2})	Biomass allocation ratio[c]	Ratio of dead biomass to live biomass[b]
Shrub	*Larrea tridentata*, *Fouquieria splendens*, *Krameria grayi*	40	13.2	Cover = AGB/1586	209.1	0.18 (leaf) 0.57 (stem) 0.25 (root)	0.2 (leaf) 0.2 (stem) 0.2 (root)
Sub- shrub	*Ambrosia deltoidea*, *Ambrosia dumosa*, *Encelia farinosa*	25	8.2	Cover = AGB/744	61.3	0.22 (leaf) 0.54 (stem) 0.24 (root)	0.1 (leaf) 0.5 (stem) 0.2 (root)
Perennial grass	*Pleuarphis rigida*, *Pennisetum setaceum*	10	3.3	Cover = AGB/ 240	7.9	0.63 (leaf) 0.37 (root)	1.3 (leaf) 2.0 (root)
Forb	*Baileya multiradiata*, *Dimorphocarpa wislizenii*	15	4.9	Cover = 0.01AGB + 2.3 × 10^{-5}AGB[b]	0.2	–	–
C3 winter annual	*Daucus pusillus*, *Plantago fastigiata*	7	2.3	Cover = 0.01AGB + 2.3 × 10^{-5}AGB[b]	0.1	–	–
C4 summer annual	*Tidestromia*, *lanuginosa Pectis papposa*	3	1.0	Cover = 0.01AGB + 2.3 × 10^{-5}AGB[b]	0	–	–

The average vegetation cover of the area was 32.9% (sample size = 30 plots with a size of 30 m × 30 m).

[a] Relative cover of FT_i = ground cover of FT_i/ground cover of all FTs (data from Camp, 1986).

[b] The plant cover-biomass relations were adopted from the original PALS-FT model (Reynolds et al., 2000).

[c] Derived from Chew and Chew (1965).

litter pools by multiplying the total litter with their respective relative proportions for leaves, stems, and roots as used in the original PALS-FT model. Average SOM was estimated from the field survey data, and its relative organic C content (0.13%) was converted to C (g) per unit area (m^2) based on soil bulk density (1.25 g cm^{-3}) and rooting depth (100 cm). This resulted in an average soil organic C of 1625 g C m^{-2} in the *Larrea-Ambrosia* community ($N = 30$ plots). The partitioning of the total soil organic C into the different SOM pools was determined as in the CENTURY model (Parton et al., 1988; Parton et al., 2001). All the above site-specific parameters are listed in Table A.1. Most of the ecophysiological parameters were determined based on literature and the original PALS-FT model, which was used to analyze the effect of rainfall variability on the hydrologic cycle of the Chihuahuan Desert ecosystem (Reynolds et al., 2000). The values of these parameters are listed in Table A.2.

4. Model evaluation

Model evaluation usually refers to verification and validation, but may also include model calibration and sensitivity analysis (Swartzman and Kaluzny, 1987; Rykiel, 1996). Model verification is performed to ascertain the correctness of the mathematical formalism and computer code, whereas model validation is the process of evaluating the consistency and accuracy of model behavior against observations (Jorgensen, 1986), or a demonstration that a model, within its domain of applicability, possesses a satisfactory range of accuracy consistent with the intended application of the model (Rykiel, 1996). Because the overall model structure and belowground components have been tested elsewhere (e.g. Reynolds et al., 1997, 2000; Kemp et al., 2003), the emphasis here is to evaluate the accuracy of the PALS-FT prediction of ANPP of a typical Sonoran Desert ecosystem against field observations. We emphasize two validation criteria: 1) the agreement between the simulated and observed ANPP for different FTs and the entire ecosystem, and 2) the agreement between the simulated and known seasonal and inter-annual patterns of ANPP in response to precipitation fluctuations. Because available field observations on NPP of arid or semiarid ecosystems are aboveground NPP, we show only simulated aboveground NPP, although the PASL-FT model simulates belowground NPP as well.

4.1. ANPP at the FT and ecosystem levels

To assess the accuracy of predicted ANPP at both the FT and ecosystem levels, we first conducted simulations for an independent test site, a *Larrea tridentata*-dominated plant community in the San Simon Valley, southeastern Arizona (Fig. 4), where detailed field measurements of ANPP are available. The San Simon Valley site is representative of the widespread *Larrea*-dominated communities of the Sonoran Desert, and similar to our study site northwest of Phoenix in terms of both community structure and soil properties (Table 2). In a 9.3 ha plot, Chew and Chew (1965) estimated the growth rate of *L. tridentata* as the addition of new nodes and its productivity as the product of the per-individual growth rate and the number of individuals for different age classes from June, 1958 to August, 1959. The aboveground productivity of other shrubs (e.g. *Parthenium incanum*) and grass species was also measured similarly.

We ran the model at a daily time step with the initial values of plant biomass for different functional types based on Chew and Chew (1965) (Table A.3) and the actual meteorological data from the San Simon Valley weather station for the same time period that the field measurements were made. Total soil organic C was estimated as 2600 g C m^{-2} a based on Kenneth's (1980) investigation on the bulk density and SOM content in the San Simon Valley area (Table 2), and was partitioned into different SOM pools as described in Section 2.4 (values listed in Table A.3). Other model input parameters, including all ecophysiological parameters, are kept the same as in Table A.2. The simulated and observed ANPP for the San Simon Valley test site showed reasonable agreement for different FTs and the community as a whole (Fig. 5a). The relative error of the simulated ANPP was ±2.4% for the whole community, and generally less than 25% for different FTs (Fig. 5b). Note that we used winter grass here, including perennial grass, forb, and C3 winter annuals, to represent the "fall crop" in Chew and Chew (1965).

For the study area in northwestern Phoenix where direct field measurements of ANPP are not available, we compared the model-predicted results with those in the literature. The simulations were conducted for

Table 2
Comparison of climatic, soil and vegetation conditions between the northwestern Phoenix study area and the San Simon Valley test site

	Northwestern phoenix	San Simon valley	Sources
Climate			
Weather stations and their locations	Waddell 33° 37′ 05″ N. Lat. 112° 27′ 35″ W. Long.	San Simon 32° 16′ N. Lat. 109° 13′ W. Long.	AZMET and
Elevation (m)	407	1100	WRCC*
Mean annual air temperature (°C)	22.2	16.8	
Mean maximum air temperature (°C)	30.2	26.6	
Mean minimum air temperature (°C)	13.7	6.8	
Annual precipitation (mm)	221.7	244.4	
Soil			
Type	Tremant Gravelly sandy loams	Kimbrough gravelly fine sandy loams	Kenneth, 1980
Depth (cm)	80–150	40–60	
Bulk density ($g\,cm^{-3}$)	1.25	1.30	Camp, 1986
Clay content (%)	12.6	17.4	
Volumetric water content (%)	7.5–11	10–17	
Soil organic matter (%)	0.23	1.0	
Plant community			
Community type	*Larrea*	*Larrea*	MacMahon, 2000 Chew and Chew, 1965
Coverage (% of surface)	25.1	20.7	
Density (number of individuals/ha)	448 (*Larrea*), 84 (*Ambrosia*), 144 (cacti)	446 (*Larrea*), 134 (other shrubs)	
Dominated species	*Larrea tridentata, Ambrosia deltoidea*	*Larrea tridentata*	
Other shrub or cacti species	*Baccharis sarothroides, Fouquieria splendens, Encelia farinosa Acacia greggii*	*Flourensia cernua, Parthenium incanum, Opuntia phaeacantha, Acacia greggii*	
Perennial grasses	*Pleuraphis rigida*	*Tridens pulchellus, Muhlenbergia porteri, Bahia absinthifolia*	

AZMET denotes the Arizona Meteorological Network, and WRCC the Western Regional Climate Center.

15 years using actual daily meteorological data from 1 January 1988 to 31 December 2002. During the 15 years, annual precipitation fluctuated between 61.8 mm (1999) and 516.5 mm (1992) (Fig. 6a). Initial conditions of the *Larrea-Ambrosia* ecosystem are listed in Tables A.1 and A.2. The simulated 15-year average ANPP of the ecosystem was $72.3\,g\,m^{-2}\,y^{-1}$, ranging from 11.3 to $229.6\,g\,m^{-2}\,y^{-1}$ (Fig. 6a). The simulated mean ANPP was quite close to the observed value ($70\,g\,m^{-2}\,y^{-1}$) suggested by Whittaker and Likens (1973) for desert scrub communities (also see Ludwig, 1987). The variability in simulated ANPP also is within the range of 10–$250\,g\,m^{-2}\,y^{-1}$ estimated by Lieth (1973) for desert scrub ecosystems and close to that of 30–$200\,g\,m^{-2}\,y^{-1}$ estimated by Noy-Meir (1973) for arid ecosystems.

Our modeling results showed that the mean ANPP of the *Larrea* ecosystem was lower in northwestern Phoenix than in southeastern Arizona. This is consistent with observations. For example, Whittaker and Niering (1975) reported that the ANPP of a *Larrea* community near Tucson, Arizona was $92.0\,g\,m^{-2}\,y^{-1}$, while Chew and Chew's (1965) field measurements showed that the ANPP of the same plant community type, located 140 km away from Tucson, could reach $130\,g\,m^{-2}\,y^{-1}$. Furthermore, the simulations showed that 70.9% of the total ecosystem ANPP was contributed by *Larrea*, 10.9% by subshrub, 3.2% by perennial grasses, 8.1% by C3 annuals, 4.0% by forbs, and 2.9% by C4 annuals. These simulated results were similar to the measurements by Chew and Chew (1965), which showed that the relative ANPP contributions

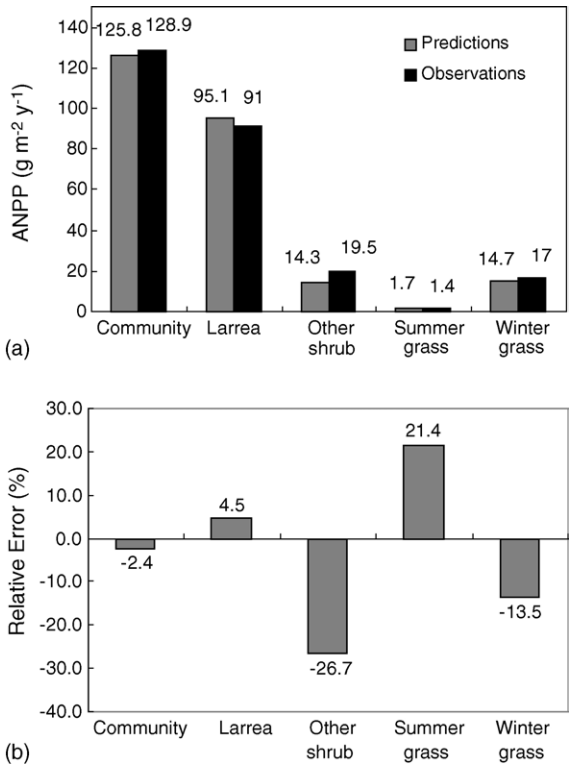

Fig. 5. Comparison of simulated aboveground net primary production (ANPP) with observed ANPP of different plant functional types of the *Larrea* ecosystem in the San Simon Valley, southeastern Arizona. Observed ANPP is from Table 7 in Chew and Chew (1965). Values are noted above each bar.

by different FTs were 69.5% for *Larrea*, 14.9% for other shrubs, 13.0% for fall crops, and about 1.1% for summer grasses (perennial grasses and forbs were not distinguished in their study).

4.2. Seasonal and inter-annual pattern of NPP in response to precipitation fluctuations

Water availability is the primary determinant of primary productivity in arid ecosystems around the world. Can the PALS-FT model accurately simulate the seasonal and inter-annual ANPP dynamics of the Sonoran Desert ecosystem in response to precipitation fluctuations? To address this question, we further analyze the responses of ANPP to precipitation changes based on our simulations at the Phoenix study area from 1988 to 2002.

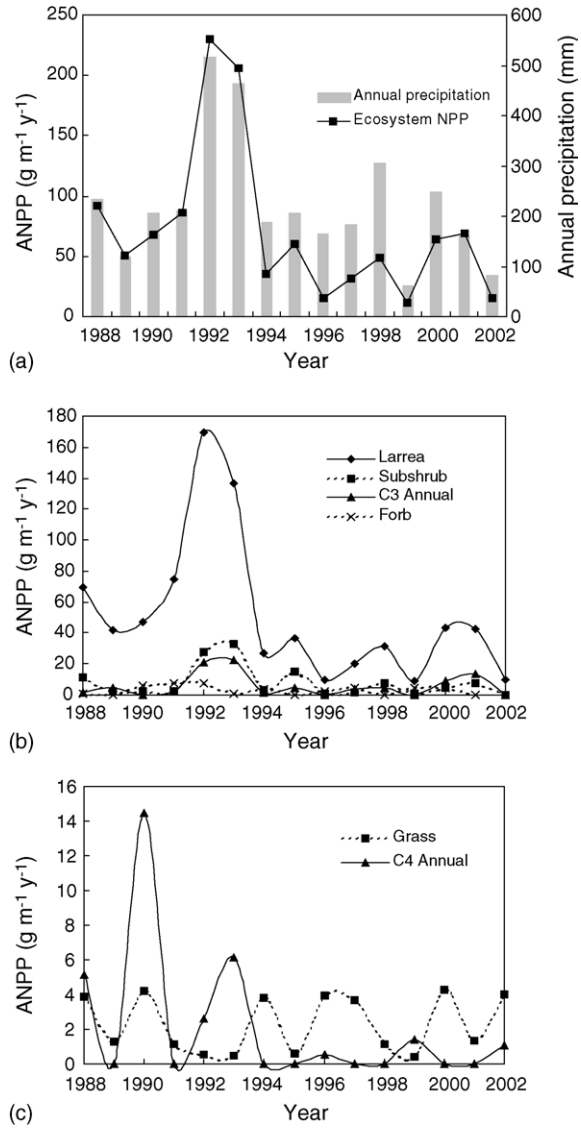

Fig. 6. Simulated decadal dynamics of ANPP of 6 plant functional types in the *Larrea* ecosystem of the Sonoran Desert Northwest of Phoenix.

Our simulation results showed that the dynamics of the ecosystem ANPP was closely related to variations in annual precipitation ($R^2 = 0.84$; Fig. 6a). At the FT level, the ANPP of shrub, subshrub, C3 winter annual and forbs also was highly correlated with annual precipitation ($R^2 = 0.80, 0.77, 0.66$, and 0.64, respectively; Fig. 6b). In contrast, the ANPP of C4 summer annuals and perennial grass did not follow the pattern of

rainfall ($R^2 = 0.11$ and 0.06, respectively; Fig. 6c). In spite of the general agreement between the two, for a particular year the relationship of ANPP with annual precipitation may not be strong. For example, while the annual precipitation in 2000 and 2001 was quite different (249.25 mm in 2000 versus 161.25 mm in 2001), the simulated ANPP for the two years was quite similar (64.6 g/m^2 in 2000 and 69.3 g/m^2 in 2001). The reason was that the leaf biomass within the ecosystem model decreased dramatically in 2000 because of the drought in 1999 with only 61 mm of rainfall. This phenomenon was also observed in the field (Bamberg et al., 1976).

How did the seasonal distribution of rainfall affect ANPP? Did the seasonal pattern of ANPP as predicted by PALS-FT agree with existing knowledge? To address these questions, we portioned annual precipitation into three parts as in Reynolds et al. (2004) (Fig. 7): spring rainfall (April 1–June 31), summer rainfall (July 1–September 31), and winter rainfall (October 1–March 31). Our analysis showed that ANPP of shrub, subshrub, C3 winter annual and forb were most closely related to winter rainfall ($R^2 = 0.68$), whereas ANPP of C4 summer annual grass was most closely related to summer rainfall ($R^2 = 0.50$). This general pattern was evident by visually comparing Figs. 7 and 8. In contrast, ANPP of perennial grasses was not strongly correlated with either annual rainfall or rainfall associated with one particular season. Fig. 7 shows that most of the precipitation in the Sonoran Desert falls in winter. This seasonal distribution pattern favors the FTs of shrubs, subshrubs, C3 annuals and forbs whose growth occurs mostly in winter (Fig. 8). However, actual growth responses of C4 grasses may be somewhat different from the modeled responses since the model parameterization for C4 grass that was based on black grama (*Bouteloua eriopoda*), which is not the dominant C4 grass in the northwestern CAP-LTER study area. The C4 grasses of this region could have phenology patterns and growth responses that are substantially different from black grama.

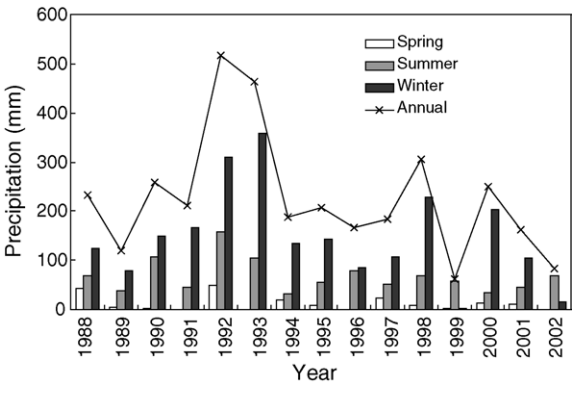

Fig. 7. Seasonal distribution and amount of rainfall in the 15 years from 1988 to 2002 in the Sonoran Desert of Northwestern Phoenix. The three seasons are defined as: spring (April 1–June 31), summer (June 30–September 30), and winter (October 1–March 31).

4.3. Comparison of simulated ANPP between PALS-FT and regression models

Comparing the predictions by different models for same ecosystem may also provide confidence in the target model. For this reason, we chose two regression models from the literature that have been used to calculate ANPP of desert ecosystem; both developed for North American hot deserts. One is the Turner and Randall's (1989) model, which is a simple regression model that considers only annual precipitation as the determining variable of desert ANPP. The other is the Webb et al. (1983) model, which considers both abiotic factors (annual precipitation, annual potential evapotranspiration) and the current standing crop as primary determinants of Desert ANPP. The Turner and Randall's model has the form:

$$\mathrm{ANPP} = 0.30 \times \mathrm{ppt} - 6.12 \tag{28}$$

where ppt is the annual rainfall in mm. The Webb et al. model has the form:

$$\mathrm{ANPP} = 1.8 \times \mathrm{FSC} \times \sum_{1}^{52} 2^{T_i/10} \times \sinh(0.1 \times \max(0, \mathrm{PPT} - \mathrm{PET}) \times \Delta t_i) \tag{29}$$

where FSC is the foliar standing crop (g/m^2), T_i the weekly average temperature (°C), sin h the hyperbolic sine function, PPT is weekly precipitation (mm), PET is potential evapotranspiration (mm), Δt_i the fraction of a year. FSC was derived from Table A.3, T_i and PPT was calculated from the weather data acquired from the San Simon Valley Weather Station. PET was calculated using the equations provided in Webb et al. (1983).

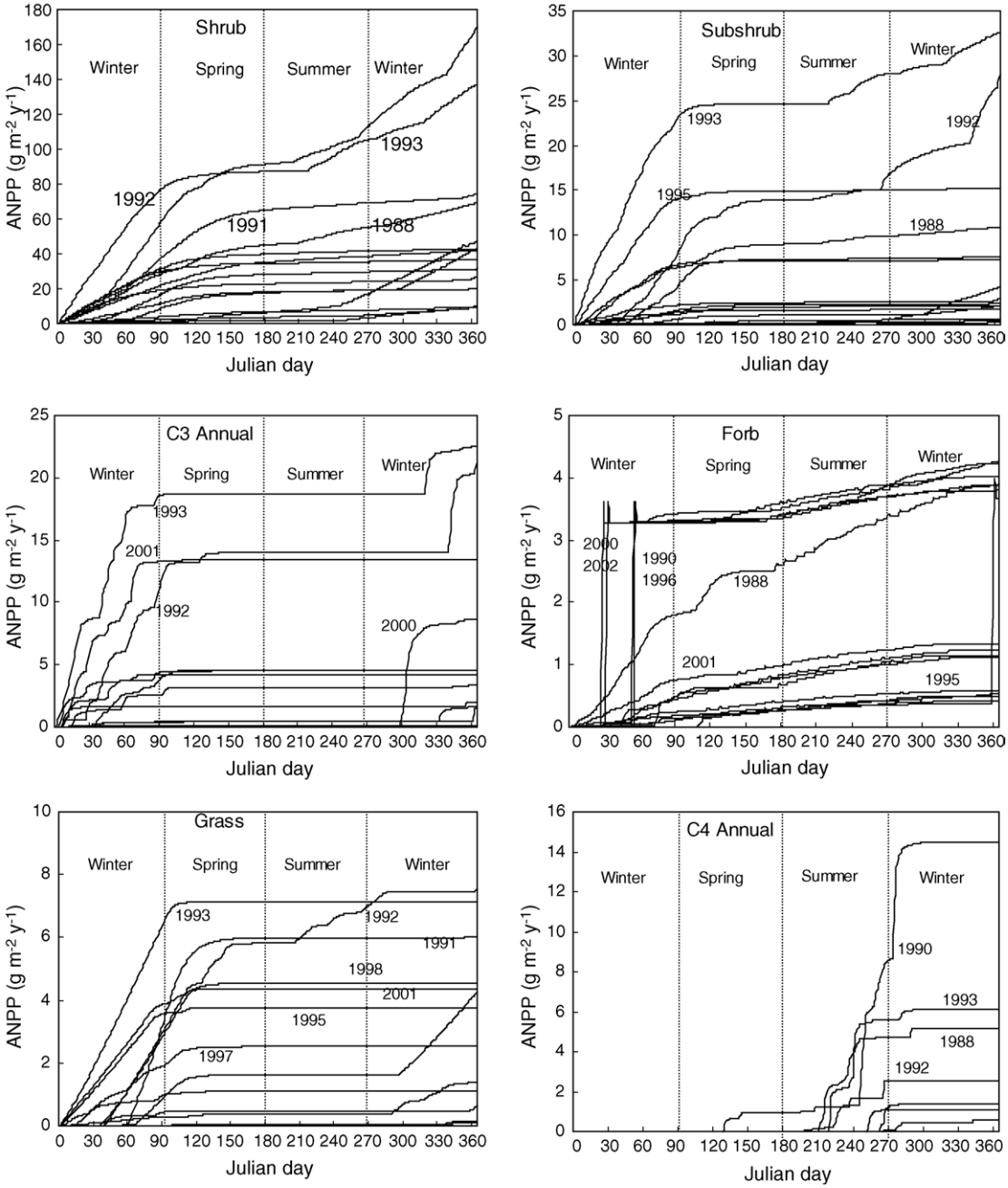

Fig. 8. Simulated seasonal variation in ANPP of different plant functional types over 15 years (1988–2002). Only those years with high rates of ANPP are shown; years having ANPP = 0 are not plotted.

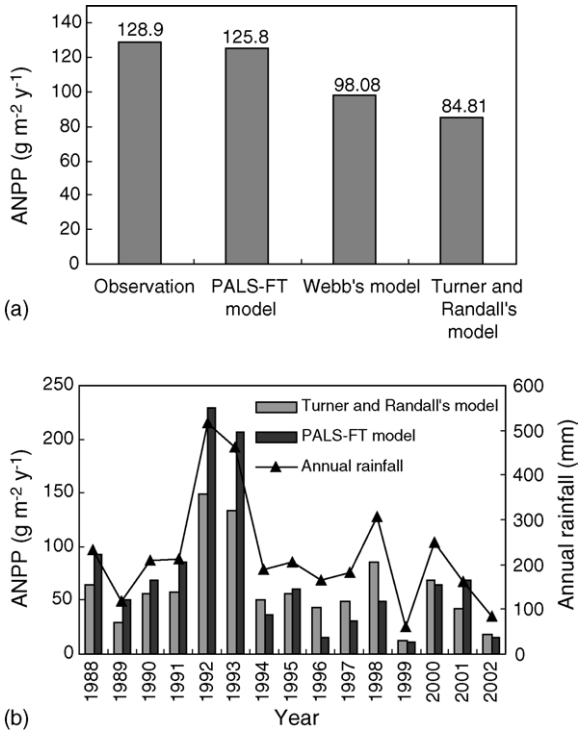

Fig. 9. Comparison of model predictions between PALS-FT and two regression models for the North American hot deserts. Panel a is for ANPP of the *Larrea* ecosystem in the San Simon Valley test site, and panel b is for ANPP of the *Larrea* ecosystem in the CAP area.

The results of the regression models are presented in comparison with PALS-FT in Fig. 9. Both regression models underestimated the *Larrea* ecosystem ANPP of the San Simon Valley test site by 23.9% and 34.2%, respectively, whereas the PALS-FT model provided an estimate that was closest to the observed ANPP (Fig. 9a). Comparing predictions of inter-annual variation in ANPP for the Larrea ecosystem in the CAP LTER study area, the Turner and Randall model prediction is more closely related to annual precipitation than the PALS-FT model prediction (Fig. 9b). However, the Turner and Randall model largely underestimates ANPP in wet years (e.g. 1992, 1993) and overestimates ANPP in very dry years (e.g. 1996, 1999; Fig. 9b). We did not use the Webb's model to simulate the inter-annual ANPP variation because it requires an observed annual FSC value, which was unavailable for the CAP study area.

5. Discussion and conclusions

The results of this study showed that the PALS-FT model, although originally developed for the Chihuahuan Desert, was able to simulate ANPP of the *Larrea*-dominated Sonoran Desert ecosystem reasonably well with only slight modifications. For the independent test site in the San Simon Valley, the relative error of the simulated ANPP was ±2.4% at ecosystem level and generally less than 25% for individual FTs. Parton et al. (1993) claimed that a relative error of ±25% should be acceptable for such simulations. The mean and variability of the simulated NPP for our Phoenix study area were also consistent with observations reported in the literature.

Simulated seasonal and inter-annual dynamics of ANPP also seemed reasonable for the Sonoran Desert ecosystem. At the ecosystem level, responses of simulated ANPP to fluctuations in annual precipitation confirmed the well documented general relationship between ANPP and precipitation in arid and semi-arid systems, as well as the high variability in productivity with respect to variability in annual rainfall (LeHouerou et al., 1988). Further examination of the relationship for individual FTs revealed the importance of the seasonal distribution of rainfall to ANPP. In particular, winter rainfall was the better predictor of ANPP for most FTs in the Sonoran Desert ecosystem, except for C4 annuals, which are more responsive to summer rainfall. This suggests that, although the decadal pattern of ANPP can be adequately predicted by that of annual precipitation, information on the seasonal distribution of rain is needed for accurate predictions of the ecosystem ANPP for particular years.

Reynolds et al. (2004) conducted a comprehensive simulation analysis to explore how plants respond to variations in precipitation and soil water availability in the three North America warm deserts. They concluded that the "pulse-reserve" model, which relates ANPP linearly to annual precipitation (Noy-Meir, 1973; Turner and Randall, 1989; Whitford, 2002), is not adequate. The simulation results of Reynolds et al. (2004) showed that rainfall characteristics (e.g. seasonality and forms of rainfall) and soil water availability were also important to plant growth. In addition to rainfall and soil water availability, several other factors such as N availability, plant age, soil properties, and resource heterogeneity also can play a major role in

determining ANPP (Whitford, 2002). Rainfall seasonality is a particularly important driving variable, as it accounts for much of the difference among the North American warm deserts and is likely to be sensitive to CO_2-induced climate change (Grimm and Fisher, 1992; Grimm et al., 1997). The results of our study further support the notion that rainfall seasonality is crucial to plant growth in the Sonoran Desert.

The comparison of predictions of the PALS-FT model with those of two published regression models showed that the PALS-FT model was more accurate in predicting ANPP of the *Larrea* ecosystem. The underestimation of ANPP by the two regression models was likely due to the exclusion of other important variables that may be influential for predicting ANPP, such as precipitation seasonality and event duration, intensity of storm depth, time lapse since last rainfall, and seasonal temperatures (Whitford, 2002). Regression models have the advantage of fewer parameter requirements, but process-based models such as PALS-FT have more predictive and explanatory power, especially in investigating ecosystem responses to climatic and environmental changes. The PALS-FT model has a structure and includes functional relationships that are similar to some other models that have been employed for analyses in semi-arid grassland ecosystem, such as the CENTURY (Parton et al., 1988, 1993) and GRASS model (Coughenour et al., 1984). The PALS-FT model offers advantages over these models for use in arid shrublands with a diversity of plant FTs, since it has greater detail with respect to soil water dynamics and includes detailed growth and phenology processes of a variety of co-occurring and competing plant functional types that are likely to be found in communities of the hot deserts of southern Arizona.

The adaptation and validation of PALS-FT at the local ecosystem level within the Sonoran Desert is a critical, but only first, step toward achieving our long-term goal of understanding how Sonoran Desert ecosystems respond to changes in environmental conditions caused by urbanization and climate change (Wu and David, 2002). Testing model predictions against field observations and other model predictions is only part of the model evaluation process, and a good agreement between simulated and measured values alone does not guarantee the correctness of the model. To further employ the PALS-FT model in the diverse central Arizona Phoenix region, three challenges must be overcome. First, additional FTs (e.g. trees, agricultural crops) that characterize other land-use and land-cover types (e.g. residential urban area, agricultural land, and the upland subdivision of the Sonoran Desert (see Fig. 4) need to be incorporated into the model, or the FTs in the current version of the PALS-FT model need to be modified, reparameterized, and validated. Second, appropriate spatially explicit simulation approaches and scaling methods must be identified and used to link landscape pattern and ecosystem processes at multiple spatial scales (e.g. local ecosystem, landscape, and the whole CAP region), correspondingly, a multilayer spatial database needs to be developed for storing and updating pattern and process information at different scales. Third, variables that show large changes associated with urbanization or climate change- for example, rising temperature, elevated atmospheric CO_2 concentration, and increasing N deposition- must be manipulated in simulation experiments to evaluate their effects. Our results confirm that such simulation experiments are likely to provide a strong and realistic set of predictions with which to compare actual long-term change in this rapidly urbanizing region. Thus, this study provides a basis for further investigating how urbanization-induced environmental changes influence the functional processes of the native Sonoran Desert ecosystem.

Acknowledgements

We would like to thank Corinna Gries and Diane Hope for their assistance with the 200-point survey data and comments on an earlier version of the manuscript, and Alaxander Buyantuyev for creating the map of the study area. This research was supported partly by U.S. EPA's STAR program (R827676-01-0 to JW), U.S. NSF (DEB 97-14833 and DEB-0423704 to CAP-LTER), and Natural Science Foundation of China (30100021 to WS and 30028002 to JW). PRK and JFR acknowledge NSF-DEB-02-12123 and USDA Specific Cooperative Agreement 58-1270-3-070 for support of the development of PALS-FT. WS also acknowledges support from Natural Science Foundation of Guangdong Province (010551) and Heshan Open Foundation. Two anonymous reviewers and Dr. Kerry Fowler made valuable comments on the manuscript.

Appendix A

The PALS-FT model input parameters and their values used in this study (see Tables A.1–A.3).

Table A.1
Site characteristic parameters and their values

Parameter	Description	Unit	Value	Source
Soil physical and climate parameters				
$ST_{i=1–2}$	Soil thickness of layer 1–2	cm	10	200-point survey
$ST_{i=3–6}$	Soil thickness of layer 3–6	cm	20	200-point survey
$Clay_{i=1–3}$	Soil clay content (layer 1–3)	%	12.6	200-point survey
$Clay_{i=4–6}$	Soil clay content (layer 4–6)	%	12	200-point survey
Silt	Soil silt content (layer 1–6)	%	51.3	200-point survey
Sand	Soil sand content (layer 1–6)	%	36.1	200-point survey
$VWC_{i=1,4–6}$	Volumetric water content at soil layer 1 and layer 4–6	%	7.5	200-point survey
$VWC_{i=2–3}$	Volumetric soil water content at layer 2–3	%	11	200-point survey
FC	Field capacity	bar	0.25	200-point survey
Ppt	Daily precipitation	mm	1988–2002	AZMET[1]
T_{max}	Daily Maximum air temperature	°C	1988–2002	AZMET
T_{min}	Daily Minimum air temperature	°C	1988–2002	AZMET
RH	Daily Relative humidity	%	1988–2002	AZMET
Sr	Daily Solar radiation	MJ	1988–2002	AZMET
C_a	Partial pressure of Atmospheric CO_2	kPa	0.036	AZMET
Plant biomass parameters				
AGB_{wnt}	Aboveground biomass of C3 grasses	g DM m^{-2}	0.2	200-point survey
AGB_{smr}	Aboveground biomass of C4 grasses	g DM m^{-2}	0	200-point survey
AGB_{forb}	Aboveground biomass of forbs	g DM m^{-2}	0.2	200-point survey
$B_{lvs,prn}$	Leaf biomass of perennial grasses	g DM m^{-2}	7.9	200-point survey
$DB_{lvs,prn}$	Dead leaf biomass of perennial grasses	g DM m^{-2}	10.5	200-point survey
$B_{rts,prn}$	Root biomass of perennial grasses	g DM m^{-2}	13.2	200-point survey
$DB_{rts,prn}$	Dead root biomass of perennial grasses	g DM m^{-2}	26.4	200-point survey
$B_{lvs,shrb}$	Leaf biomass of shrub	g DM m^{-2}	50.4	200-point survey
$DB_{lvs,shrb}$	Dead leaf biomass of shrub	g DM m^{-2}	10.1	200-point survey
$B_{stm,shrb}$	Stem biomass of shrub	g DM m^{-2}	158.8	200-point survey
$DB_{stm,shrb}$	Dead stems of shrub	g DM m^{-2}	31.8	200-point survey
$B_{rts,shrb}$	Root biomass of shrub	g DM m^{-2}	70.6	200-point survey
$DB_{rts,shrb}$	Dead root of shrub	g DM m^{-2}	14.1	200-point survey
$B_{lvs,ss}$	Subshrub leaf biomass	g DM m^{-2}	14.8	200-point survey
$DB_{lvs,ss}$	Subshrub dead leaf biomass	g DM m^{-2}	1.5	200-point survey
$B_{stm,ss}$	Subshrub stem biomass	g DM m^{-2}	43.4	200-point survey
$DB_{stm,ss}$	Subshrub dead stem biomass	g DM m^{-2}	21.7	200-point survey
$B_{rts,ss}$	Subshrub root biomass	g DM m^{-2}	20.5	200-point survey
$DB_{rts,ss}$	Subshrub dead root biomass	g DM m^{-2}	4.1	200-point survey
Plant litter and soil organic matter parameters				
$L_{met,lvs}$	Leaf litter metabolic C	g C m^{-2}	2.5	200-point survey
$L_{str,lvs}$	Leaf litter structural C	g C m^{-2}	18.8	200-point survey
$L_{met,rts}$	Root litter metabolic C	g C m^{-2}	2.0	200-point survey
$L_{str,rts}$	Root litter structural C	g C m^{-2}	6.0	200-point survey
$L_{met,stm}$	Stem litter metabolic C	g C m^{-2}	0.5	200-point survey
$L_{str,stm}$	Stem Litter structural C	g C m^{-2}	1.5	200-point survey
AOM_{lvs}	Leaf active OM	g C m^{-2}	12.5	200-point survey
AOM_{rts}	Root active OM	g C m^{-2}	13.5	200-point survey
SOM_{rts}	Root slow OM	g C m^{-2}	725	200-point survey

Table A.1 (*Continued*)

Parameter	Description	Unit	Value	Source
POM_{rts}	Root passive OM	$g\,C\,m^{-2}$	862	200-point survey
N_{soil}	Soil nitrogen content	$g\,N\,m^{-2}$	5.74	200-point survey
$K_{met,lvs}$	Metabolic leaf litter decomposition rate	fraction	0.05	Kemp et al., 2003
$K_{met,rts}$	Metabolic root litter decomposition rate	fraction	0.05	Kemp et al., 2003
$K_{met,stm}$	Metabolic stem litter decomposition rate	Fraction	0.003	Moorhead and Reynolds, 1989
$K_{AOM,lvs}$	Leaf Active organic matter decomposition rate	Fraction	0.0016	Kemp et al., 2003
$K_{AOM,rts}$	Root active organic matter decomposition rate	fraction	0.0016	Kemp et al., 2003
$K_{SOM,rts}$	Root slow organic matter decomposition rate	fraction	0.00054	Kemp et al., 2003
$K_{POM,rts}$	Root passive organic matter decomposition rate	Fraction	0.000019	Kemp et al., 2003

Table A.2
Ecophysiological input parameters and their values used in the PALS-FT model

Parameter	Description	Value Unit	Shrub (Larrea)	Subshrub	Perennial grass	Forb	C3 annuals	C4 annuals	Source
$RF_{i=1-6}$	Root distribution fraction 0–10 cm	Fraction	0.1	0.1	0.2	0.2	0.3	0.4	Kemp et al., 1997; Thames, 1979
			0.19	0.2	0.3	0.2	0.4	0.4	Forseth et al., 1984
	10–20 cm		0.48	0.25	0.25	0.3	0.25	0.2	Reynolds et al., 2004
	20–40 cm		0.15	0.25	0.15	0.2	0.05	0	
	40–60 cm		0.05	0.2	0.10	0.1	0	0	
	60–80 cm		0.02	0	0	0	0	0	
	80–100 cm								
SLA	Specific leaf area,	$m^2\ g^{-1}$	0.006	0.011	0.015	0.015	0.015	0.015	Werk et al., 1983
Phi	Respiratory loss per day	Fraction	0.45	0.40	0.35	0.25	0.25	0.25	Reynolds et al., 2000
a	Parameter in Eq. 14	Dimensionless	0.52	0.566	0.75	1.0	1.0	0.75	Reynolds et al., 2000
b	Parameter in Eq. 14	Dimensionless	−0.06	−0.125	−0.15	−0.18	−0.20	−0.25	Reynolds et al., 2000
$C_{min,i}$	Partial pressure of intercellular CO_2	kPa	0.023	0.025	0.016	0.025	0.025	0.015	Forseth and Ehleringer, 1983; Werk et al., 1984
R_{lvs}	Ratio of production of leaves	Fraction	0.4	0.4	0.95	1.0	1.0	1.0	Reynolds et al., 2000
R_{rts}	Ratio of production of roots	Fraction	0.3	0.25	0.05	0.2	0.25	0.3	Reynolds et al., 2000
N_{max}	Maximum N content in leaf	%	3.0	4.0	2.5	4.0	4.0	3.0	Lajtha and Whitford, 1989
N_{min}	Minimum N content in leaf,	%	0.8	0.8	0.75	1.0	1.0	1.0	Lajtha and Whitford, 1989
N_{stem}	N content in stem	%	2.4	1.5	–	–	–	–	Kemp et al., 2003
N_{root}	N content in root	%	2.4	2.5	1.0	2.0	2.0	2.0	Kemp et al., 2003
$F_{lab,min}$	Fraction of N in labile material lost due to microbial respiration;	Fraction					0.55		Reynolds et al., 2000
$F_{lig,min}$	Fraction of N in non-labile material (lignin and cellulose) lost due to microbial respiration	Fraction					0.30		Reynolds et al., 2000
N_{lvs}	Nitrogen content in litter	%					2.4		Kemp et al., 2003
C_{plant}	Carbon content in plant	Fraction					0.52		Kemp et al., 2003
LG_{lvs}	Lignin content in leaf litter	Fraction					0.10		Kemp et al., 2003
CL_{lvs}	Cellulose content in leaf litter	Fraction					0.65		Kemp et al., 2003
LG_{stm}	Lignin content in stem litter	Fraction					0.22		Kemp et al., 2003
CL_{stm}	Cellulos content in stem litter	Fraction					0.53		Kemp et al., 2003
LG_{rts}	Lignin content in root litter	Fraction					0.22		Kemp et al., 2003
CL_{rts}	Cellulose content in root litter	Fraction					0.53		Kemp et al., 2003
N/C	Fixed N/C ratio	Fraction					0.0067		Kemp et al., 2003

Table A.3
List of major input parameters for the test site in San Simon Valley

Input parameters	Unit	Shrub (Larrea)	Other shrub	Perennial grass	Forb	Annual grass (mainly C3)
For different plant functional types						
Live leaf biomass	g DM m^{-2}	49.18	6.8	0.48	0.2	0.1
Dead leaf biomass	g DM m^{-2}	9.84	0.64	0.64	0	0
Live stem biomass	g DM m^{-2}	320.3	7.20	0	0	0
Dead stem biomass	g DM m^{-2}	64.05	3.60	0	0	0
Live root biomass	g DM m^{-2}	96.99	10.5	0.8	0	0
Dead root biomass	g DM m^{-2}	19.4	2.1	0.16	0	0
Root distribution (in three layers)	Fraction	0.1, 0.5, 0.4	0.3, 0.5, 0.2	0.5, 0.4, 0.1	0.4, 0.5, 0.1	0.6, 0.4, 0.0
For the whole ecosystem						
Metabolic leaf litter	g C m^{-2}	4.3				
Structural leaf litter	g C m^{-2}	32.3				
Metabolic stem litter	g C m^{-2}	0.9				
Structural stem litter	g C m^{-2}	2.7				
Metabolic root litter	g C m^{-2}	3.5				
Structural root litter	g C m^{-2}	10.5				
Surface active organic matter	g C m^{-2}	2.4				
Active soil organic matter	g C m^{-2}	78.6				
Slow soil organic matter	g C m^{-2}	1152				
Passive soil organic matter	g C m^{-2}	1378				

Biomass of *Larrea* was derived from mean standing weight of individuals (g dry matter per plant) from Chew and Chew (1965). Biomass of other FTs was estimated based on the cover values of different FTs in Chew and Chew (1965) and the cover-biomass relations listed in Table 1. Methods for determining dead biomass, biomass allocation ratios, root distribution fractions, litter and soil organic matter pools are described in text.

References

Ball, J.T., Woodrow, I.E., Berry, J.A., 1987. A model predicting stomatal conductance and its contribution to the control of photosynthesis under different environmental conditions. In: Biggens, J. (Ed.), Progress in Photosynthesis Research. Martinus-Nijhoff, Dordrecht, The Netherlands, pp. 221–224.

Bamberg, S.A., Vollmer, A.T., Kleinkopf, G.E., Ackerman, T.L., 1976. A comparison of seasonal primary production of Mojave Desert shrubs during wet and dry years. Am. Midland Naturalist 95, 398–405.

Bell, K.L., Hiatt, H.D., Niles, W.E., 1979. Seasonal changes in biomass allocation in eight winter annuals of the Mojave Desert. J. Ecol. 67, 781–787.

Brown, D.E. (Ed.), 1994. Biotic Communities: Southwestern United States and Northwestern Mexico. University of Utah Press, Salt Lake City, Utah.

Burk, J., Dick-Peddie, W.A., 1973. Comparative production of *Larrea divaricata* Cav. on three geomorphic surfaces in southern New Mexico. Ecology 54, 1094–1102.

Caldwell, M.M., Camp, L.B., 1974. Belowground productivity of two cool desert communities. Oecologia 17, 123–130.

Camp, P.D., 1986. Soil survey of Aguila-Carefree area, parts of Maricopa and Pinal Counties, Arizona. United States Department of Agriculture, Soil Conservation Service, In cooperation with United Statess Department of the Interior, Bureau of Indian Affairs and Bureau of Land Management, and the Arizona Agricultural Experiment Station.

Campbell, G.S., 1977. An Introduction to Environmental Biophysics, 2nd ed. Springer-Verlag, New York.

Chew, R.M., Chew, A.E., 1965. The primary productivity of a desert shrub (*Larrea tridentata*) community. Ecol. Monographs 35, 335–375.

Coughenour, M.B., McNaughton, S.J., Wallace, L.L., 1984. Modelling primary production of perennial graminoids: uniting physiological processes and morphometric traits. Ecol. Modelling 23, 101–134.

Ehleringer, J., 1983. Ecophysiology of *Amaranthus palmeri*, a Sonoran Desert summer annual. Oecologia 57, 107–112.

Fischer, R.A., Turner, N.C., 1978. Plant productivity in the arid and semiarid zones. Ann. Rev. Plant Physiol. 29, 277–317.

Fisher, F.M., Zak, J.C., Cunningham, G.L., Whitford, W.G., 1988. Water and nitrogen effects on growth and allocation patterns of creosotebush in the northern Chihuahuan Desert. J. Range Manage. 41, 387–390.

Forseth, I.N., Ehleringer, J., 1983. Ecophysiology of two solar tracking desert winter annuals. III. Gas exchange responses to light, CO_2 and VPD in relation to long-term drought. Oecologia 57, 340–351.

Forseth, I.N., Ehleringer, J.R., Werk, K.S., Cook, C.S., 1984. Field water relations of Sonoran Desert annuals. Ecology 65, 1436–1444.

Gao, Q., Reynolds, J.F., 2003. Historical shrub-grass transitions in the northern Chihuahuan Desert: modeling the effects of shifting rainfall seasonality and event size over a landscape gradient. Global Change Biol. 9, 1475–1493.

Grimm, N.B., Grove, J.M., Redman, C.L., Pickett, S.T.A., 2000. Integrated approaches to long-term studies of urban ecological systems. BioScience 50, 571–584.

Grimm, N.B., Fisher, S.G., 1992. Responses of arid land streams to changing climate. In: Firth, P., Fisher, S.G. (Eds.), Climate Change and Freshwater Ecosystems. Springer-Verlag, New York.

Grimm, N.B., Chacón, A., Dahm, C.N., Lind, O.T., Starkweather, P.L., Wurtsbaugh, W.W., 1997. Sensitivity of aquatic ecosystems to climatic and anthropogenic changes: the Basin and Range, American Southwest, and México. Hydrol. Process. 11, 1023–1041.

Hadley, N.F., Szarek, S.R., 1981. Productivity of desert ecosystems. BioScience 31, 747–753.

Hope, D., Gries, C., Zhu, W., Fagan, W.F., Redman, C.L., Grimm, N.B., Nelson, A.L., Martin, C., Kinzig, A., 2003. Socioeconomics drive urban plant diversity. Proc. Nat. Acad. Sci. 100, 8788–8792.

Jarvis, P.G., 1976. The interpretation of the variations in leaf water potential and stomatal conductance found in canopies in the field. Philosophical transactions of the Royal Society of London Series B. Biol. Sci. 273, 593–610.

Johnson, H.B., Vasek, F.C., Yonkers, T., 1978. Residual effects of summer irrigation on Mojave Desert annuals. Bull. California Acad. Sci. 77, 95–108.

Jorgensen, S.E., 1986. Fundamentals of Ecological Modelling. Elsevier, Amsterdam, The Netherlands.

Kemp, P.R., Reynolds, J.F., Packepsky, Y., Chen, J.-L., 1997. A comparative modeling study of soil water dynamics in a desert ecosystem. Water Resources Res. 33, 73–90.

Kemp, P.R., Reynolds, J.F., Virginia, R.A., Whitford, W.G., 2003. Decomposition of leaf and root litter of Chihuahuan desert shrubs; effects of three years of summer drought. J. Arid Environ. 53, 21–39.

Kenneth, D.V., 1980. Soil survey of San Simon area, Arizona, parts of Cochise, Graham, and Greenlee Counties. United States Department of Agriculture, Soil Conservation Service in cooperation with Arizona Agricultural Experiment Station.

Lajtha, K., Whitford, W.G., 1989. The effect of water and nitrogen amendments on photosynthesis, leaf demography, and resource-use efficiency in *Larrea tridentata*, a desert evergreen shrub. Oecologia 80, 341–348.

LeHouerou, H.N., Bingham, R.L., Skerbek, W., 1988. Relationship between the variability of primary production and the variability of annual precipitation in world arid lands. J. Arid Environ. 15, 1–18.

Leuning, R., 1995. A critical appraisal of a combined stomatal-photosynthesis model for C3 plants. Plant Cell Environ. 18, 339–355.

Lieth, H., 1973. Primary production: terrestrial ecosystems. Human Ecol. 1, 303–332.

Ludwig, J.A., 1986. Primary production variability in desert ecosystems. In: Whitford, W.G. (Ed.), Pattern and Process in Desert Ecosystems. University of New Mexico Press, Albuquerque, New Mexico, USA, pp. 5–17.

Ludwig, J.A., 1987. Primary productivity in arid lands: myths and realities. J. Arid Environ. 13, 1–7.

MacMahon, J.A., 2000. Warm deserts. In: Barbour, M.G., Billings, W.D. (Eds.), North American Terrestrial Vegetation. Cambridge University Press, Cambridge, UK, pp. 285–322.

Monteith, J.L., Unsworth, M.H., 1990. Principles of Environmental Physics, 2nd ed. Edward Arnold, New York.

Moorhead, D.L., Reynolds, J.F., 1989. The contribution of abiotic processes to buried litter decomposition in the northern Chihuahuan Desert. Oecologia 79, 133–135.

Noy-Meir, I., 1973. Desert ecosystems: environment and producers. Ann. Rev. Ecol. Systematics 4, 25–51.

Oren, R., Sperry, J.S., Katul, G.G., Pataki, D.E., Ewers, B.E., Phillips, N., Schäfer, K.V.R., 1999. Survey and synthesis of intra- and interspecific variation in stomatal sensitivity to vapor pressure deficit. Plant Cell Environ. 22, 1515–1526.

Parton, W.J., Stewart, W.B., Cole, C.V., 1988. Dynamics of C, N, P and S in grassland soils: a model. Biogeochemistry 5, 109–131.

Parton, W.J., Scurlock, J.M.O., Ojima, D.S., Gilmanov, T.G., Scholes, R.J., Schimel, D.S., Kirchner, T., Menaut, J.-C., Seastedt, T., Garcia Moya, E., Kamnalrut, A., Kinyamario, J.I., 1993. Observations and modeling of biomass and soil organic matter dynamics for the grassland biome worldwide. Global Biogeochem. Cycles 7, 785–809.

Parton, W.J., Coughenour, M.B., Scurlock, M.O., Ojima, D.S., Gilmanov, T.G., Scholes, R.J., Schimel, D.S., Kirchner, T.B., Menaut, J.-C., Seastedt, T.R., Moya, E.G., Kamnalrut, A., Kinyamario, J.I., Hall, D.O., 1996. Global grassland ecosystem modeling: development and test of ecosystem models for grassland systems. In: Breymeyer, A.T., Hall, D.O., Mellillo, J.M., Agren, G.I. (Eds.), SCOPE 56: Global Change Effects on Coniferous Forests and Grasslands. John Wiley & Sons, New York, pp. 229–268.

Parton, B., Ojima, D.S., Grossoand, S.D., Keough, C., 2001. CENTURY tutorial: supplement to CENTURY user's manual. Great Plains System Research Unit Technical Reprot no. 4, US-DA-ARS, Fort Collins, Colorado, USA.

Reynolds, J.F., Cunningham, G.L., 1981. Validation of a primary production model of the desert shrub *Larrea tridentata* using soil-moisture augmentation experiments. Oecologia 51, 357–363.

Reynolds, J.F., Hilbert, D.W., Kemp, P.R., 1993. Scaling ecophysiology from the plant to the ecosystem: A conceptual framework. In: Ehleringer, J.E., Field, C.B. (Eds.), Scaling Physiological Process. Academic Press, San Diego, pp. 127–140.

Reynolds, J.F., Kemp, P.R., Ogle, K., Fernandez, R.J., 2004. Precipitation pulses, soil water and plant responses: modifying the 'pulse-reserve' paradigm for deserts of North America. Oecologia 141, 194–210.

Reynolds, J.F., Kemp, P.R., Tenhunen, J.D., 2000. Effects of long-term rainfall variability on evapotranspiration and soil water distribution in the Chihuahuan Desert: a modeling analysis. Plant Ecol. 150, 145–159.

Reynolds, J.F., Smith, D.M.S. (Eds.), 2002. Global Desertification: Do Humans Cause Deserts?. Dahlem University Press, Berlin.

Reynolds, J.F., Strain, B.R., Cunningham, G.L., Knoerr, K.R., 1980. Predicting primary production for forest and desert ecosystem models. In: Hesketh, J.D., Jones, J.W. (Eds.), Predicting Photosynthesis for Ecosystem Models. CRC Press, Boca Raton, Florida, pp. 160–207, Vol. II.

Reynolds, J.F., Virginia, R.A., Schlesinger, W.H., 1997. Defining functional types for models of desertification. In: Smith, T.M., Shugart, H.H., Woodward, F.I. (Eds.), Plant Functional Types: Their Relevance to Ecosystem Properties and Global Change. Cambridge University Press, Cambridge, pp. 195–216.

Ruimy, A., Saugier, B., Dedieu, G., 1994. Methodology for the estimation of terrestrial net primary production from remotely sensed data. J. Geophys. Res. 99, 5263–5383.

Ryan, M.G., Hunt Jr., E.R., McMurtrie, R.E., Agren, G.I., Aber, J.D., Friend, A.D., Rastetter, E.B., Pulliam, W.M., Raison, R.J., Linder, S., 1996. Comparing models of ecosystem function for temperate conifer forests. I. Model description and validation. In: Breymeyer, A.T., Hall, D.O., Mellillo, J.M., Agren, G.I. (Eds.), SCOPE 56: Global Change Effects on Coniferous Forests and Grasslands. John Wiley & Sons, New York, pp. 313–362.

Rykiel Jr., E.J., 1996. Testing ecological models: the meaning of validation. Ecol. Modelling 90, 229–244.

Schlesinger, W.H., Reynolds, J.F., Cunningham, G.L., 1990. Biological feedbacks in global desertification. Science 247, 1043–1048.

Shreve, F., 1951. Vegetation and Flora of the Sonoran Desert. Volume I. Vegetation. Carnegie Institute of Washington Publication no. 591.

Shugart, H.H., 1984. A Theory of Forest Dynamics: The Ecological Implications of Forest Succession Models. Springer-Verlag, New York.

Swartzman, G.L., Kaluzny, S.P., 1987. Ecological Simulation Primer. MacMillan Publishing, New York.

Thames, J.L., 1979. Tucson validation site report. US/IBP Desert Biome Research Memorandum 77-3. In: Final Progress Reports, Validation Studies. Utah State University, Logan, Utah.

Tiktak, A., van Grinsven, H.J.M., 1995. Review of sixteen forest-soil-atmosphere models. Ecol. Modelling 83, 35–53.

Turner, F.B., Randall, D.C., 1989. Net production by shrubs and winter annuals in Southern Nevada. J. Arid Environ. 17, 23–26.

Turner, R.M., Brown, D.E., 1994. Sonoran desertscrub. In: Brown, D.E. (Ed.), Biotic Communities: Southwestern United States and Northwestern Mexico. University of Utah Press, Salt Lake City, pp. 181–221.

Webb, W.L., Szarek, S.R., Lauenroth, W.K., Kinerson, R.S., Smith, M., 1978. Primary productivity and water use in native forest, grassland, and desert ecosystems. Ecology 59, 1239–1247.

Webb, W.L., Lauenroth, W.K., Szarek, S.R., Kinerson, R.S., 1983. Primary production and abiotic controls in forests, grasslands, and desert ecosystems in the United States. Ecology 64, 134–151.

Werk, K.S., Ehleringer, J., Forseth, I.N., Cook, C.S., 1983. Photosynthetic characteristics of Sonoran Desert winter annuals. Oecologia 59, 101–105.

Whitford, W.G., 2002. Ecology of Desert Systems. Cambridge University Press, Cambridge, UK.

Whittaker, R.H., Likens, G.E., 1973. Primary production: the biosphere and man. Human Ecol. 1, 357–369.

Whittaker, R.H., Niering, W.A., 1975. Vegetation of the Santa Catalina mountains, Arizona. V. Biomass, production, and diversity along the elevation gradient. Ecology 56, 771–790.

Wu, J., 2001. Desertification. In: Robinson, R. (Ed.), Plant Sciences. Macmillan Reference USA, New York.

Wu, J., David, J.L., 2002. A spatially explicit hierarchical approach to modeling complex ecological systems: theory and applications. Ecol. Modelling 153, 7–26.

Wu, J., Levin, S.A., 1994. A spatial patch dynamic modeling approach to pattern and process in an annual grassland. Ecol. Monographs 64, 447–464.

Wu, J., Levin, S.A., 1997. A patch-based spatial modeling approach: conceptual framework and simulation scheme. Ecol. Modelling 101, 325–346.